

MoS₂ quantum dots-based optical sensing platform for the analysis of synthetic colorants. Application to quinoline yellow determination

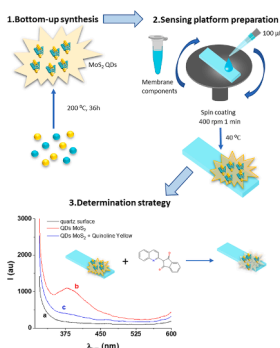
Rut Martínez-Moro, María del Pozo, Elena Casero, María Dolores Petit-Domínguez*, Carmen Quintana*

Departamento de Química Analítica y Análisis Instrumental. Facultad de Ciencias. c/ Francisco Tomás y Valiente, N°7. Campus de Excelencia de la Universidad Autónoma de Madrid, 28049 Madrid, Spain

HIGHLIGHTS

- MoS₂-QDs incorporated as fluorophore into the matrix of PVC membranes.
- MoS₂-QDs@PVC/quartz sensing platform for food additives determination.
- MoS₂-QDs fluorescence inhibition by quinoline yellow.

GRAPHICAL ABSTRACT



ARTICLE INFO

Keywords:

MoS₂ quantum dots
Hydrothermal synthesis
Fluorescence quenching
Quinoline yellow
Optical sensor

ABSTRACT

In this work, a novel fluorescence sensor has been designed to solve the actual need of new fast and inexpensive sensing platforms for the analysis of synthetic colorants. It is based on MoS₂ quantum dots obtained by a hydrothermal method and incorporated as fluorophore into the matrix of PVC membranes, which are deposited on quartz substrates by spin-coating. It was proven, as in these conditions, MoS₂ quantum dots maintain the fluorescent properties that they present in solution. Experiments carried out in solution displayed a maximum emission when they were excited under 310 nm. This initial fluorescence decreases linearly in presence of increasing concentrations of various synthetic colorants namely quinoline yellow, tartrazine, sunset yellow, allura red, ponceau 4R and carmoisine. The two possible mechanisms that can explain this quenching effect, colorants absorbing photons emitted by quantum dots and/or competing with the nanomaterial for photons coming from the excitation source, were evaluated. The most pronounced effect was observed with quinoline yellow, as a result of a mixed mechanism. The optimized methodology developed for the determination of quinoline yellow showed a linear concentration range between 5.4 and 55.0 µg with a limit of detection of 1.6 µg. The sensor was applied to the determination of quinoline yellow in a food colour paste obtaining results in good agreement with those obtained by HPLC-UV-vis measurements.

* Corresponding authors.

E-mail addresses: mdolores.petit@uam.es (M.D. Petit-Domínguez), carmen.quintana@uam.es (C. Quintana).

1. Introduction

Colorants can be found in many food products since they improve its appearance, making them more attractive to customers [1]. Most used food colorants are classified as natural or synthetic depending on its origin. Originally, natural colorants obtained from plants and animals were applied until the middle of the nineteenth century [2]. These were replaced by synthetic colorants since they are cheaper and present better stability [3,4]. Among these compounds, the most used in industry present organic rings and/or azo- ($N=N$) groups in their chemical structures (allura red, quinoline yellow, tartrazine, sunset yellow and carmoisine to name a few). Recent studies have shown a relation between long-term consumption of products containing synthetic food colorants and several health issues such as allergies, children hyperactivity, asthmatic reactions and even cancer [5–7]. Therefore, it is of great importance to control and establish safe levels of these compounds in foods. Different techniques are used in the analysis of food colorants, including thin layer chromatography [8] (TLC), capillary electrophoresis [9], electrochemistry [10] and mainly high performance liquid chromatography [11,12] (HPLC). However, some of these popular and reliable techniques are time-consuming, expensive, require complex sample pre-treatment and/or involve sample destruction. In recent years, spectroscopic methods have gained attention for the detection of various analytes including synthetic food colorants. Surface-enhanced Raman spectroscopy (SERS) has attracted the interest of many researchers as it is a fast, sensitive, and inexpensive detection method¹ that has been successfully applied in synthetic food colorants analysis showing promising results [6,13,14]. Fluorescence and UV–vis spectroscopy using different fluorescent probes have been used in many studies for the detection of food colorants [15,16].

Since the discovery of graphene, low dimensional materials have experimented a ground-breaking expansion due to its unique and outstanding properties. Beyond carbon materials, which have been exhaustively studied, researchers focused their efforts on the study of layered materials with structures similar to graphite such as transition metal dichalcogenides (TMDs) [17]. They present the general formula MX_2 , where M represents a transition metal from group IV, V or VI, and X a chalcogen like Se, Te or S, covalently bonded in a sandwich-like structure. Conformed by multiple layers stacked by van der Waals interactions, they can be easily exfoliated into lower dimension materials such as nanosheets (2D) and quantum dots (0D) that present different mechanical, optical and electronic properties [18]. Among TMDs, MoS_2 has been the centre of attention in the past decade partly due to its relative abundance in nature [19,20]. Several studies proved the successful application of MoS_2 nanosheets in the development of new sensors for the detection of a high variety of analytes, alone or combined with other nanomaterials [21–23]. However, MoS_2 quantum dots (MoS_2 -QDs) did not received the same attention until recently.

Unlike 2D nanosheets, MoS_2 -QDs present intrinsic fluorescent properties [24] which make them excellent candidates in the development of optical based sensors. Actually, several studies have already proved its applicability in the detection of various analytes [25,26] including food colorants [16]. MoS_2 -QDs preparation can be classified in two major groups: top-down and bottom-up. Top-down strategies are mainly based on the exfoliation of the bulk materials into thin layers for example by the solvothermal method [27], via liquid-phase exfoliation [28] or Li intercalation [29], while bottom-up strategies use Mo and S precursors followed by heat treatment (hydrothermal method) [30].

In this study, experiments conducted in solution proved that the initial fluorescence of MoS_2 -QDs decreases in the presence of various synthetic colorants, and that this change in intensity shows a linear relation with increasing concentrations, being the most pronounced effect with quinoline yellow (QY). Considering the actual need of new fast and inexpensive sensing platforms for the analysis of synthetic colorants, we have designed a novel sensor based on MoS_2 -QDs included in an optical transparent membrane. After immobilization, QDs

maintain its fluorescent properties that are quenched as a consequence of the addition of quinoline yellow. Finally, this novel sensor has been successfully applied on a real sample of pastry colorant to determine its QY content.

2. Materials

2.1. Reagents

Quinoline yellow, sunset yellow, ponceau 4R, carmoisine, allura red, tartrazine, poly (vinyl chloride) (PVC), tributyl phosphate and L-cysteine were purchased from Sigma Aldrich (USA). Sodium molybdate was obtained from Panreac Química S.L.U (Spain). Sodium acetate, sodium hydroxide, acetonitrile, sulphuric acid and acetic acid, and tetrahydrofuran (THF) were purchased from Scharlab (Spain). Water was purified with a Millipore Milli-Q-System (Burlington, Massachusetts, USA). All solutions were prepared just before use.

Paste food colour yellow (PME cake, England, UK) was employed as real sample for analytical applications.

2.2. Instrumentation

A vacuum-free Ossila spin coater was used for homogeneously spread on top of quartz plaques the suspension containing the membrane components and the MoS_2 -QDs. Membrane thickness was evaluated in 5 different points with a Dektak 3030ST profilometer with nanometric vertical resolution.

For the MoS_2 -QDs synthesis, an ultrasound bath (Transonic 570/H Elma), a pH-meter 827 from Metrohm (Herisau, Switzerland) for pH adjustment, an Eppendorf centrifuge 5804 (Hamburg, Germany) and a Nabertherm Iberica (Spain) furnace were used.

Both, a spectrophotometer Shimadzu UV-1800 and a spectrofluorometer Hitachi F-7000 with a solid sample holder (650-0161) were employed for optical measurements.

High Performance Liquid Chromatography (HPLC) measurements were performed with a Jasco Analytica PU-1580 high pressure pumping system, equipped with an injector Rheodyne Model 7125, a 20 μ L loop and a Kromasil C18 column (150 \times 4.6 mm; 5 μ m; Scharlau). A Perkin Elmer 785A UV/VIS was employed as detector of the chromatographic system.

3. Experimental

3.1. MoS_2 -QDs synthesis

MoS_2 -QDs were obtained using a previously described hydrothermal method with slight modifications [31]. 0.3 g $Na_2MoO_4 \cdot 2H_2O$ and 0.9 g L-cysteine were dissolved in 10 mL of distilled water. After agitation for 30 min, pH was adjusted to 6.5 using 0.1 M HCl, and distilled water was added until a volume of 20.0 mL was reached. The solution was then transferred to a Teflon-lined stainless-steel autoclave and subjected to heat treatment at 200 °C for 36 h. After centrifugation at 11,000 rpm for 30 min supernatant was collected and kept at 4 °C until use.

3.2. MoS_2 -QDs based optical sensor preparation.

The optical transparent membrane containing the MoS_2 -QDs was prepared as follows: 35 mg of high molecular weight poly (vinyl chloride) contained in an Eppendorf were dissolved in 790 μ L of tetrahydrofuran. Subsequently, 100 μ L of hydrothermal MoS_2 quantum dots and 110 μ L of tributyl phosphate were added. After each addition the mixture was stirred employing a vortex. Once the mixture containing the QDs is ready, 100 μ L of it are deposited on top of a quartz plaque and homogeneously dispersed under optimized conditions (400 rpm for 1 min) using a spin coater. Finally, the sensing platform (MoS_2 -QDs @PVC/quartz) was let dry in an oven under 40 °C until dryness. For

blank measurements, membranes without MoS₂-QDs were prepared in the same way. Before the modification, the quartz plaques were successively cleaned with THF, H₂SO₄ 0.2 M, NaOH 0.2 M, and finally rinsed with distilled water.

The addition of standard solutions of quinoline yellow or sample was carried out by drop casting the appropriate volumes and letting dry again in the oven.

3.3. Spectroscopic measurements

The as-synthesized MoS₂-QDs were characterized by spectroscopic measurements performed in solution. Absorbance and fluorescence spectra were recorded with a 1 cm quartz cuvette in both cases.

For spectrofluorometric measurements, the MoS₂-QDs@PVC/quartz platform was placed in the solid sample holder. After evaluating different excitation wavelengths, 310 nm was selected as λ_{ex} to conduct further experiments with a slit of 5.0 nm.

3.4. Chromatographic measurements

HPLC-UV experiments were performed at a flow rate of 0.8 mL min⁻¹, employing a mixture of 0.025 M sodium acetate/acetic buffer of pH 6.00 and acetonitrile (85:15, v/v) as mobile phase. A wavelength of 414 nm was employed for detection. In these conditions, quinoline yellow can be detected at a retention time (t_R) of 2.60 min.

3.5. Sample preparation

For optical measurements, the analysis of the sample was performed by standard addition as follows: 480 mg of paste food colour yellow (PME cake, England, UK) were dissolved in 10 mL of distilled water. Aliquots of 100 μ L of this solution, non-spiked and spiked with increasing concentrations of QY, were diluted to 5.00 mL in a volumetric flask. Finally, 100 μ L of this solution was placed on top of the MoS₂-QDs@PVC/quartz sensor and then let dry in the oven.

For HPLC-UV analysis, external calibration method was employed. In this case, an accurate amount around 60 mg of the sample (56.7 mg as average of 3 replicates) were dissolved in 25.0 mL of distilled water. Samples were diluted 1:200 with the mobile phase and filtered through a 0.45 μ m pore size nylon filter before to be injected in the chromatographic system.

4. Results and discussion

4.1. Nanomaterial characterization

UV-vis spectra of MoS₂-QDs obtained by hydrothermal method was registered after a 1:100 dilution in distilled water. As shown in Fig. 1A two peaks can be identified at 275 and 320 nm which have been previously described. According to bibliography, these would correspond to electronic transitions of π to π^* and n to π^* , respectively [26]. The absence of further peaks at longer wavelengths evidences the absence of nanosheets since 2D MoS₂ presents four absorption peaks in the 390–680 nm range [32].

Emission spectra of MoS₂-QDs under different excitation wavelengths around the maxima λ of absorption (275 and 320 nm) were registered as can be seen in Fig. 1B. Graphs show an emission band around 390 nm (λ_{em}), being the maximum emission for at λ_{ex} of 310 nm, hence it was selected as optimum wavelength for further experiments. Since band at 390 nm remains almost constant with λ_{ex} , it can be concluded that no dispersion in size or highly edge oxidation of the as-synthesized QDs are produced [33–35].

4.2. Effect of food dyes on MoS₂-QDs fluorescence

The interaction between MoS₂-QDs and several synthetic dyes that are very popular in food industry, namely quinoline yellow, tartrazine, sunset yellow, allura red, ponceau 4R and carmoisine, was evaluated. Fig. 2A shows the comparison of emission spectrum of QDs and the absorption spectra of selected colorants.

Different degrees of overlapping are observed depending on the colorant. In particular, for tartrazine and QY, the overlap of their absorption band and the emission band of the QDs is maxima. On the other hand, the degree of overlapping between the absorption band of each colorant and the λ_{ex} of the QDs, marked with a vertical line in the Fig. 2A, is highly dependent on the colorant itself. Therefore, it is reasonable to think that all dyes will induce a decrease of MoS₂-QDs emission but not in the same extend. In order to confirm this, fluorescence of the MoS₂-QDs (1:600 diluted in distilled water) was registered in the absence and in presence of a fixed concentration of $2 \cdot 10^{-5}$ M of each dye. As observed in Fig. 2B, all colorants induced a decrease, in a greater or lesser extent, of the initial fluorescent signal, verifying our initial hypothesis.

To further characterize the interaction between MoS₂-QDs and each colorant, experiments were carried out to determine Stern-Volmer constants (K_{SV}) [32], a parameter that enables to quantitatively

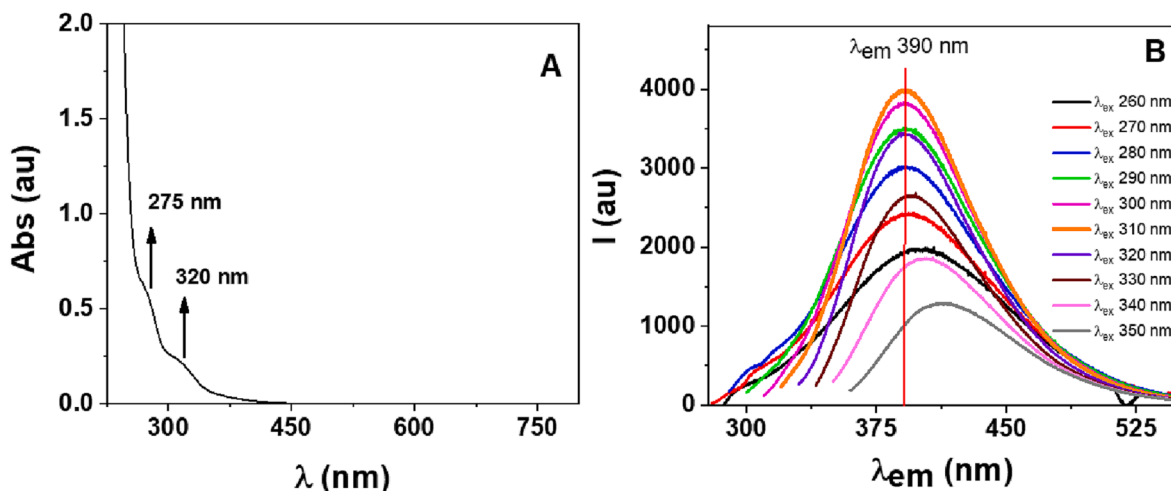


Fig. 1. A) Absorption spectra of MoS₂-QDs obtained by hydrothermal method B) Emission spectra of MoS₂-QDs registered under different λ_{ex} ranging from 260 to 350 nm.

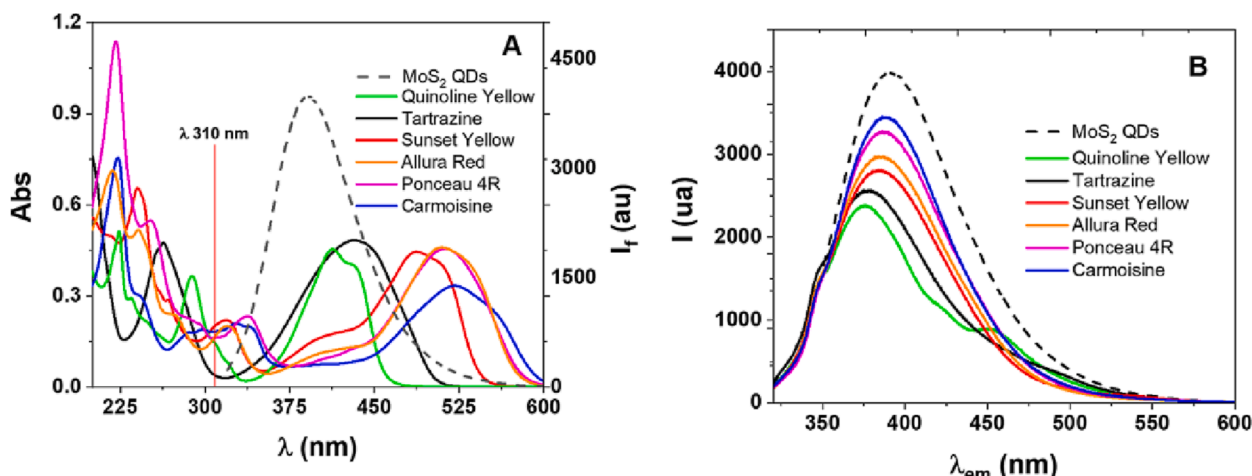


Fig. 2. A) MoS₂-QDs emission spectra at λ_{ex} 310 nm (indicated with a vertical line) and absorption spectra of all colorants tested in the study. B) Emission spectra of 1:600 diluted MoS₂-QDs in absence and in presence of different synthetic dyes with $2 \cdot 10^{-5}$ M concentration.

evaluate the degree of interaction between fluorophore and quencher and which is calculated through the same name equation (equation (1)):

$$\frac{I_f}{I_0} = 1 + K_{SV}[Q] \quad (1)$$

Where I_0 and I_f correspond to emission intensity of MoS₂-QDs in absence and in the presence of the different dyes, respectively; K_{SV} is the corresponding Stern-Volmer constant, and Q represents the synthetic colorant concentration. The higher the value of K_{SV} , the higher the interaction is. To this purpose, MoS₂-QDs emission intensities were measured in the presence of increasing contents of each synthetic dye, showing a linear response as can be seen in Fig. 3.

The K_{SV} obtained for the interaction of each colorant with the as-synthesized MoS₂-QDs are summarized in Table 1. As can be observed, QY presents the strongest interaction. Hence, it was selected as analyte in the following experiments.

4.3. Interaction between MoS₂-QDs and QY

Additional studies were carried out to further understand how QDs and quinoline yellow interacted. Fig. 4A shows the absorption spectrum

of QY (green spectrum) and the emission spectra of MoS₂-QDs excited at 310 nm (red spectrum) and 335 nm (blue spectrum). As previously mentioned, for λ_{ex} 310 nm, QY not only absorbs light at 310 nm excitation wavelength but also can absorb photons emitted by MoS₂-QDs due to an overlap in both spectra. However, at λ_{ex} 335 nm the absorption of QY is minimum. If a quenching of the nanomaterial fluorescence is produced in presence of QY when exciting at 335 nm, the absorption of the photons emitted by the QDs should be the inhibition mechanism instead of the competition for the photons coming from the excitation source. Hence, in order to elucidate which mechanism is predominant, emission spectra of MoS₂-QDs in absence and in presence of different concentrations of QY were registered at both λ_{ex} (Fig. 4B). The percentage of initial intensity (I_0) maintained in presence of QY was calculated as % $I_0 = (I_f/I_0) \cdot 100$, being I_f the fluorescence intensity measured with each concentration of colorant, at both excitation wavelengths. In Fig. 4B are depicted the results of these experiments, showing that, irrespective to the λ_{ex} employed, inhibition is produced. Therefore, the quenching observed at 335 nm demonstrated the inhibition mechanism due to the overlap of the spectra. Moreover, as inhibition at λ_{ex} 310 nm is greater than at 335 nm, we can conclude that fluorescence inhibition at this condition would be due to a mixed mechanism where quinoline yellow not only absorbs photons emitted by MoS₂-QDs but also competes with the nanomaterial to absorb light coming from the excitation source.

4.4. Response of the MoS₂-QDs @PVC/quartz sensor towards QY

Once the interaction MoS₂-QDs and QY has been demonstrated, efforts were focused on developing an optical sensing platform taking advantage of the luminescence properties of the nanomaterial. To this end, quartz plaques, employed as substrate, were pre-treated and modified with the MoS₂-QDs as described in *Experimental Procedures* section. Analysis of the thickness of the PVC membranes revealed that MoS₂-QDs@PVC membranes are thinner and more homogeneous ($3.1 \pm 0.2 \mu\text{m}$) than that prepared without MoS₂-QDs ($6 \pm 2 \mu\text{m}$).

Fig. 5 shows the emission spectra of the quartz substrate (a), and the quartz surface modified with MoS₂-QDs in the absence (b) and in the presence of QY (c). As can be observed, once the MoS₂-QDs are immobilized through the membrane on the quartz surface, they maintain its fluorescent properties. After the addition of QY (150 μL by drop casting) a decrease in the fluorescence response was clearly observed demonstrating that the interaction with the colorant also takes place when studies on surface are accomplished.

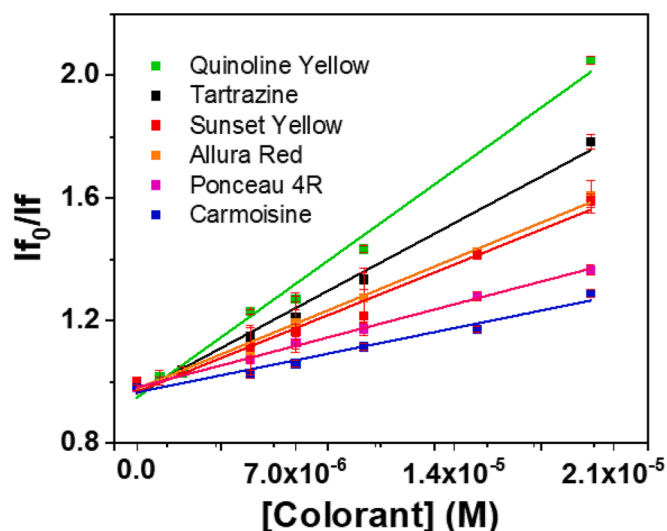
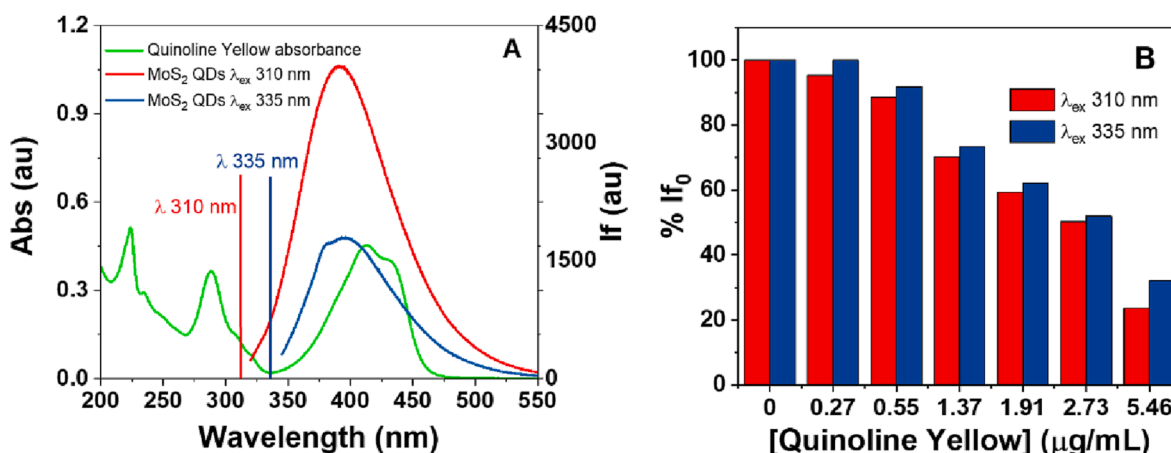
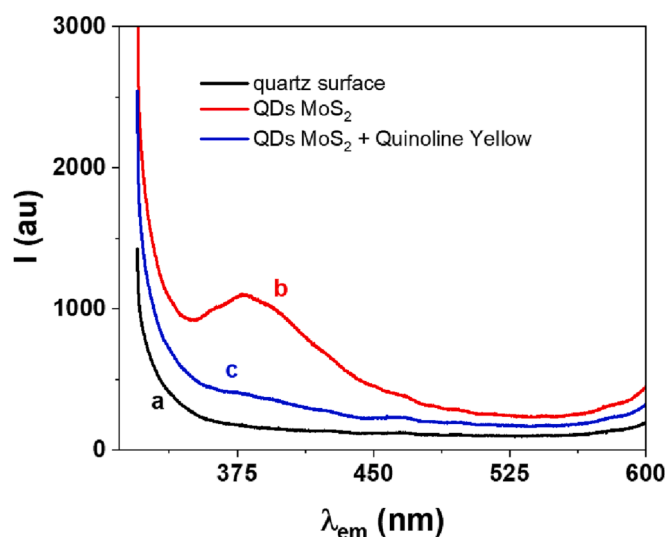


Fig. 3. Fluorescence inhibition of MoS₂-QDs with increasing concentrations of synthetic colorants. All measurements were performed under λ_{ex} 310 nm and data taken at λ_{em} 390 nm as it was explained in optical characterization section.

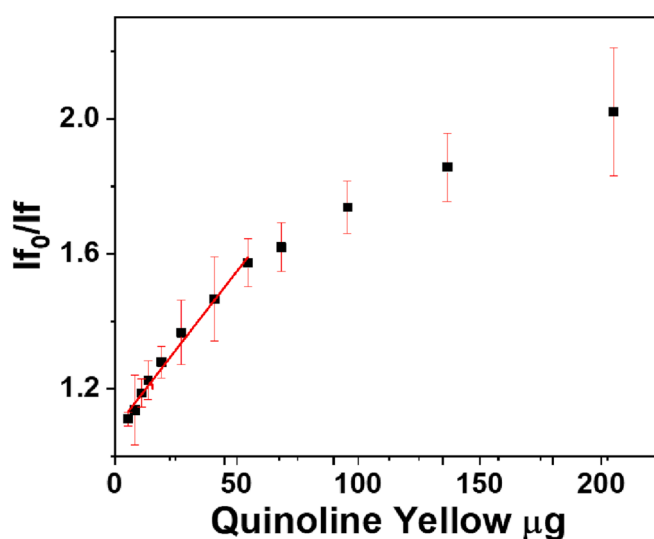
Table 1Stern-Volmer constants of the interaction between MoS₂-QDs and selected colorants.

Colorant	Quinoline Yellow	Tartrazine	Sunset Yellow	Allura Red	Ponceau 4R	Carmoisine
K _{SV} (M ⁻¹)	55,294	40,944	32,361	32,343	19,376	16,921

**Fig. 4.** A) Absorption spectra of QY and emission spectra of MoS₂-QDs at λ_{ex} of 310 nm and 335 nm. B) % of If₀ MoS₂ QDs maintained in presence of increasing concentrations of QY at λ_{ex} of 310 nm and 335 nm.**Fig. 5.** Emission spectra at λ_{ex} 310 nm of a) quartz surface, b) MoS₂-QDs @PVC/quartz sensor, c) MoS₂-QDs @PVC/quartz sensor + 150 μL of 275 $\mu\text{g/mL}$ QY.

4.5. Influence of QY concentration on the analytical response

The fluorescence response of the MoS₂-QDs@PVC/quartz sensor after deposition of 100 μL of solutions containing increasing amounts of QY was evaluated and the results are displayed in Fig. 6. As can be observed, as QY amount increases, higher inhibition of the QDs fluorescence is produced. Note that in this case, as the QY is being dried before measuring the final fluorescence signal, the content added is expressed in mass units (μg) instead of concentration. A linear response was observed between 5.4 and 55.0 μg , according to the equation $I_{\text{f0}}/I_{\text{f}} = (1.08 \pm 0.01) + (9.3 \pm 0.6) \cdot 10^{-3} \mu\text{g}$, $r = 0.990$ (see Fig. 6). Limits of detection ($3\sigma/\text{slope}$) and quantification ($10\sigma/\text{slope}$) of 1.6 and 5.4 μg were obtained, respectively. Precision was also evaluated at different concentrations levels in the linear range obtaining relative standard deviation values lower than 9.1% ($n = 5$).

**Fig. 6.** MoS₂-QDs@PVC/quartz sensor response with increasing content of QY. λ_{ex} 310 nm, λ_{em} 390 nm. 100 μL of QY solution deposited on top of the sensor surface by drop casting.

4.6. Real sample measurements: QY determination

Application of the method to real samples was evaluated on a food colour paste. Content of quinoline yellow was determined by the standard addition method, by drop-casting non-spiked and spiked samples (see sample preparation section) on the sensor surface. As observed in Fig. 7A, inhibition increases linearly with increasing content of QY added, following the equation: $I_{\text{f0}}/I_{\text{f}} = (1.62 \pm 0.05) + (8.2 \pm 0.6) \cdot 10^{-2} \mu\text{g}$, $r = 0.992$. Values obtained for the non-spiked sample higher than 1 for $I_{\text{f0}}/I_{\text{f}}$ prove the presence of the colorant as indicated in the label. A medium percentage of $(21 \pm 1)\%$ of quinoline yellow was found in the product with RSD lower than 7%.

The results obtained with this new sensing platform were compared with that obtained by HPLC-UV-vis detection following a previously described procedure [12]. In the conditions described in the

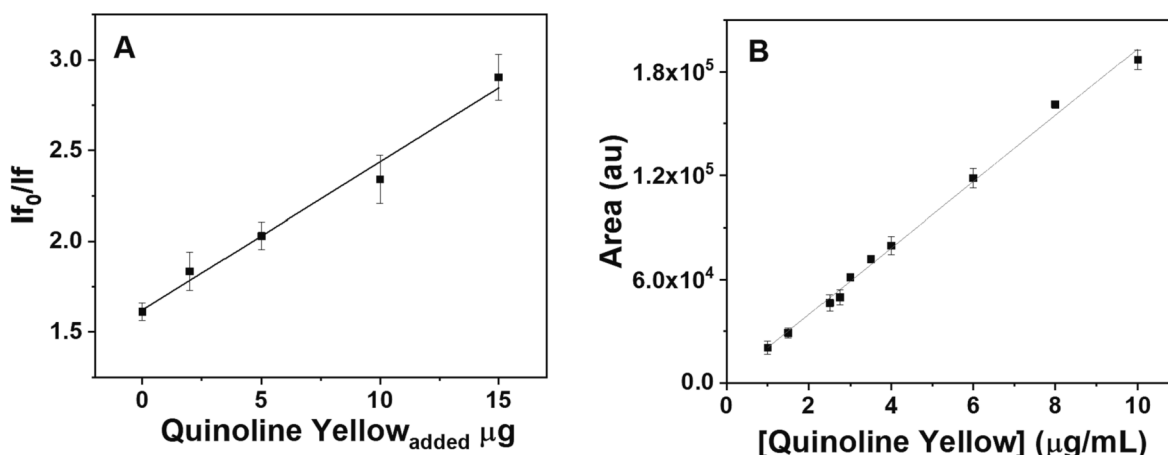


Fig. 7. A). Calibration plot corresponding to the standard addition determination of QY in paste food colour yellow. Fluorescence emission data was obtained under λ_{ex} 310 nm and λ_{em} 390 nm. B) HPLC-UV-vis calibration curve measured at t_R 2.60 min and with UV-vis detection at 414 nm. $Q = 0.8$ mL/min. (For interpretation of the references to colour in this figure legend, the reader is referred to the web version of this article.)

Experimental section, QY was detected at a retention time (t_R) of 2.6 min. By increasing QY concentration, a calibration curve between 1 and 10 $\mu\text{g/mL}$, (Fig. 7B) was obtained according to $\text{Area (a.u)} = (1.4 \pm 0.3) \times 10^3 + (1.92 \pm 0.05) \times 10^4 [\text{QY}] (\mu\text{g/mL})$ and $r = 0.998$. By the interpolation of the area registered for the sample diluted 1:200 in mobile phase, $(4.49 \pm 0.01) \times 10^4$, we obtain a quinoline yellow concentration of 2.27 $\mu\text{g/mL}$ that represents a 20 % of the total mass in the sample ($n = 3$), with an RSD of 2 %. These data are in good agreement with those obtained by applying the MoS_2 -QDs based sensor described in this article.

5. Conclusions

MoS_2 -QDs were synthesized by a hydrothermal method and incorporated through optical transparent PVC membranes on quartz plaques (MoS_2 -QDs@PVC/quartz) giving rise to a novel fluorescence sensor for the determination of synthetic colorants in food. It was proven that the synthesized MoS_2 -QDs present native fluorescence, with a maximum of emission at 390 nm when they are excited at 310 nm, which is maintained after immobilization on a solid support. The interaction between MoS_2 -QDs with all the colorants tested (carmoisine, ponceau 4R, allura red, sunset yellow, tartrazine, quinoline yellow) cause a decrease in the initial MoS_2 -QDs fluorescence. The calculated Stern-Volmer constant, ranging from 16,921 to 55,294 M^{-1} , demonstrated that the strongest interaction takes place for QY. In this case, we conclude that the inhibition of the initial fluorescence is due to a mixed mechanism in which QY absorbs both photons emitted by MoS_2 -QDs and light coming from the excitation source in clear competition with the nanomaterial. The fluorescence response of the MoS_2 -QDs@PVC/quartz sensor was evaluated towards increasing QY amounts, founding a linear concentration range between 5.4 and 55.0 μg with a limit of detection of 1.6 μg and a relative standard deviation lower than 9.1% ($n = 5$). Finally, the sensor was applied to the determination of QY in a food colour paste with good results that were confirmed by HPLC measurements.

CRedit authorship contribution statement

Rut Martínez-Moro: Investigation, Validation, Visualization Writing - review & editing. **María del Pozo:** Methodology, Formal analysis. **Elena Casero:** Conceptualization, Writing - review & editing, Project administration, Funding acquisition. **María Dolores Petit-Domínguez:** Conceptualization, Supervision, Writing - review & editing, Funding acquisition. **Carmen Quintana:** Conceptualization, Supervision, Writing - original draft, Project administration, Funding acquisition.

Declaration of Competing Interest

The authors declare that they have no known competing financial interests or personal relationships that could have appeared to influence the work reported in this paper.

Data availability

Data will be made available on request.

Acknowledgment

The authors acknowledge financial support from projects PID2020-113142RB-C22 funded by MCIN/AEI/ 10.13039/501100011033 and P2018/NMT-4349 (TRANSNANOAVANSENS-CM) funded by the Comunidad Autónoma de Madrid. We thank A. Redondo and D. García for the profilometer measurements.

References

- [1] Y. Yao, W. Wang, K. Tian, W.M. Ingram, J. Cheng, L. Qu, H. Li, C. Han, Highly reproducible and sensitive silver nanorod array for the rapid detection of Allura Red in candy, *Spectrochim. Acta, Part A* 195 (2018) 165–171.
- [2] V. Sharma, H.T. McKone, P.G. Markow, A global perspective on the history, use, and identification of synthetic food dyes, *J. Chem. Educ.* 88 (2011) 24–28.
- [3] F. Karimi, E. Demir, N. Aydogdu, M. Shojaei, M.A. Taher, P.N. Asrami, M. Alizadeh, Y. Ghasemi, S. Cheraghi, Advancement in electrochemical strategies for quantification of Brown HT and Carmoisine (Acid Red 14) from azo dyestuff class, *Food Chem. Toxicol.* 165 (2022), 113075.
- [4] R. Dai, Y. Hu, Green/red dual emissive carbon dots for ratiometric fluorescence detection of acid red 18 in food, *Sens. Actuators, B* 370 (2022), 132420.
- [5] N. Khorshidi, A. Niazi, A novel ion pair based surfactant assisted microextraction modified by orthogonal signal correction partial least squares for determination of food dyes, *J. Food Meas. Charact.* 12 (2018) 1885–1895.
- [6] Y. Ou, X. Wang, K. Lai, Y. Huang, B.A. Rasco, Y. Fan, Gold nanorods as surface-enhanced Raman spectroscopy substrates for rapid and sensitive analysis of Allura Red and Sunset Yellow in beverages, *J. Agric. Food Chem.* 66 (2018) 2954–2961.
- [7] H. Alp, D. Başkan, A. Yaşar, N. Yaylı, Ü. Ocak, M. Ocak, Simultaneous determination of sunset yellow FCF, allura red AC, quinoline yellow WS, and tartrazine in food samples by RP-HPLC, *J. Chem.* (2018).
- [8] F.I. De Andrade, M.I.F. Guedes, I.G.P. Vieira, F.N.P. Mendes, P.A.S. Rodrigues, C.S. C. Maia, M.M.M. Avila, L.M. Ribeiro, Determination of synthetic food dyes in commercial soft drinks by TLC and ion-pair HPLC, *Food Chem.* 157 (2014) 193–198.
- [9] J. Yi, L. Zeng, Q. Wu, L. Yang, T. Xie, Sensitive simultaneous determination of synthetic food colorants in preserved fruit samples by capillary electrophoresis with contactless conductivity detection, *Food Anal. Methods* 11 (2018) 1608–1618.
- [10] S.M. Ghoreishi, M. Behpour, M. Golestaneh, Simultaneous determination of Sunset yellow and Tartrazine in soft drinks using gold nanoparticles carbon paste electrode, *Food Chem.* 132 (2012) 637–641.

- [11] R. Li, Y. Wang, J. Tan, S.H. Tang, Z.T. Jiang, S. Di, Y. Geng, Simultaneous determination of synthetic edible pigments in beverages by titania-based RP-HPLC, *Arab. J. Chem.* 13 (2020) 3875–3881.
- [12] Ş.D. Zor, B. Aşçı, Ö.A. Dönmez, D.Y. Küçükkaraca, Simultaneous determination of potassium sorbate, sodium benzoate, quinoline Yellow and Sunset Yellow in lemonades and lemon sauces by HPLC using experimental design, *J. Chromatogr. Sci.* 54 (6) (2016) 952–957.
- [13] J. Neng, Q. Zhang, P. Sun, Application of surface-enhanced Raman spectroscopy in fast detection of toxic and harmful substances in food, *Biosens. Bioelectron.* 167 (2020), 112480.
- [14] L. Li, Q. Cui, M. Li, T. Li, S. Cao, S. Dong, Y. Wang, Q. Dai, J. Ning, Rapid detection of multiple colorant adulteration in Keemun black tea based on hemp spherical AgNPs-SERS, *Food Chem.* 398 (2023), 133841.
- [15] Y. Lou, W. Sun, L. Jiang, X. Fan, K. Zhang, S. Chen, Z. Li, J. Ji, J. Ou, L. Liao, A. Qin, Double-enhanced fluorescence of graphene quantum dots from cane molasses via metal and PEG modification for detecting metal ions and pigments, *Opt. Mater. (Amsterdam, Neth.)*, 133 (2022) 113037.
- [16] H. Xu, X. Yang, G. Li, C. Zhao, X. Liao, Green synthesis of fluorescent carbon dots for selective detection of Tartrazine in food samples, *J. Agric. Food Chem.* 63 (2015) 6707–6714.
- [17] B.L. Li, J. Wang, H.L. Zou, S. Garaj, C.T. Lim, J. Xie, N.B. Li, D.T. Leong, Low-dimensional transition metal dichalcogenide nanostructures based sensors, *Adv. Funct. Mater.* 26 (2016) 7034–7056.
- [18] M. Pumera, A.H. Loo, Layered transition-metal dichalcogenides (MoS₂ and WS₂) for sensing and biosensing, *TrAC, Trends Anal. Chem.* 61 (2014) 49–53.
- [19] A. Taffelli, S. Dirè, A. Quaranta, L. Pancheri, MoS₂ based photodetectors: a review, *Sensors* 21 (2021) 2758.
- [20] A. Gupta, T. Sakthivel, S. Seal, Recent development in 2D materials beyond graphene, *Prog. Mater. Sci.* 73 (2015) 44–126.
- [21] M.D. Petit-Domínguez, C. Quintana, L. Vázquez, M. del Pozo, I. Cuadrado, A. M. Parra-Alfambra, E. Casero, Synergistic effect of MoS₂ and diamond nanoparticles in electrochemical sensors: determination of the anticonvulsant drug valproic acid, *Microchim. Acta* 185 (2018) 334.
- [22] E. Blanco, L. Rocha, M. del Pozo, L. Vázquez, M.D. Petit-Domínguez, E. Casero, C. Quintana, A supramolecular hybrid sensor based on cucurbit[8]uril, 2D-molibdenum disulphide and diamond nanoparticles towards methyl viologen analysis, *Anal. Chim. Acta* 1182 (2021), 338940.
- [23] A.M. Parra-Alfambra, E. Casero, L. Vázquez, C. Quintana, M. del Pozo, M.D. Petit-Domínguez, MoS₂ nanosheets for improving analytical performance of lactate biosensors, *Sens. Actuators, B* 274 (2018) 310–317.
- [24] N.S. Arul, V.D. Nithya, Molybdenum disulfide quantum dots: synthesis and applications, *RSC Adv.* 6 (2016) 65670–65682.
- [25] Y. Fan, S. Che, L. Zhang, C. Zhou, H. Fu, Y. She, Highly sensitive visual fluorescence sensor for aminoglycoside antibiotics in food samples based on mercaptosuccinic acid-CdTe quantum dots, *Food Chem.* 404 (2023), 134040.
- [26] X. Liu, W. Zhang, L. Huang, N. Hu, W. Liu, Y. Liu, S. Li, C. Yang, Y. Suo, J. Wang, Fluorometric determination of dopamine by using molybdenum disulfide quantum dots, *Microchim. Acta* 185 (2018) 234.
- [27] S. Xu, D. Li, P. Wu, One-Pot, facile, and versatile synthesis of monolayer MoS₂/WS₂ quantum dots as bioimaging probes and efficient electrocatalysts for hydrogen evolution reaction, *Adv. Funct. Mater.* 25 (2015) 1127–1136.
- [28] Z.X. Gan, L.Z. Liu, H.Y. Wu, Y.L. Hao, Y. Shan, X.L. Wu, P.K. Chu, Quantum confinement effects across two-dimensional planes in MoS₂ quantum dots, *Appl. Phys. Lett.* 106 (2015), 233113.
- [29] W. Qiao, S. Yan, X. Song, X. Zhang, X. He, W. Zhong, Y. Du, Luminescent monolayer MoS₂ quantum dots produced by multi-exfoliation based on lithium intercalation, *Appl. Surf. Sci.* 359 (2015) 130–136.
- [30] X. Ren, L. Pang, Y. Zhang, X. Ren, H. Fan, S.F. Liu, One-step hydrothermal synthesis of monolayer MoS₂ quantum dots for highly efficient electrocatalytic hydrogen evolution, *J. Mater. Chem. A* 3 (2015) 10693–10697.
- [31] L. Hu, Q. Zhang, X. Gan, W. Yin, W. Fu, Switchable fluorescence of MoS₂ quantum dots: a multifunctional probe for sensing of chromium(VI), ascorbic acid, and alkaline phosphatase activity, *Anal. Bioanal. Chem.* 410 (2018) 7551–7557.
- [32] A. Coloma, M. del Pozo, R. Martínez-Moro, E. Blanco, P. Atienzar, L. Sánchez, M. D. Petit-Domínguez, E. Casero, C. Quintana, MoS₂ quantum dots for on-line fluorescence determination of the food additive Allura Red, *Food Chem.* 345 (2021), 128628.
- [33] W. Yin, X. Bai, X. Zhang, J. Zhang, X. Gao, W.W. Yu, Multicolor light-emitting diodes with MoS₂ quantum dots, *Part. Part. Syst. Character.* 36 (2019) 1800362.
- [34] W. Dai, H. Dong, B. Fugetsu, Y. Cao, H. Lu, X. Ma, X. Zhang, Tunable fabrication of molybdenum disulfide quantum dots for intracellular microRNA detection and multiphoton bioimaging, *Small* 11 (33) (2015) 4158–4164.
- [35] S. Pal, K.K. Tadi, P.M. Sudeep, S. Radhakrishnan, T.N. Narayanan, Temperature assisted shear exfoliation of layered crystals for the large-scale synthesis of catalytically active luminescent quantum dots, *Mater. Chem. Front.* 1 (2017) 319–325.